SIAM Rev.
Vol. 40, No. 2, pp. 356–371, June 1998

017

LITHOTRIPSY: THE TREATMENT OF KIDNEY STONES WITH SHOCK WAVES*

LAURENS HOWLE†, DAVID G. SCHAEFFER‡, MICHAEL SHEARER§, AND PEI ZHONG¶

Abstract. This paper discusses mathematical models for the response of a small air bubble in water to an ultrasound pulse, a context that arises in the modern treatment for kidney stones. The paper reviews Rayleigh's 1917 theory for bubble response, applies asymptotics to describe large-amplitude solutions of Rayleigh's equations, and briefly discusses effects neglected in the simple model. The style is expository, intended both to introduce this application to mathematicians and to illustrate the use of asymptotic methods to nonmathematicians.

Key words. shock waves, bubble dynamics, asymptotic methods

AMS subject classifications. 76Z99, 76Q05, 41A60

PII. S0036144597322630

1. Lithotripsy and bubble dynamics. Since its clinical introduction [4] in the early 1980s, millions of kidney-stone patients worldwide have been successfully treated with shock-wave lithotripsy. In this procedure, brief intense ultrasound pulses (up to 1000 atmospheres in peak pressure, lasting a few microseconds) are used to break a stone into pieces small enough to be passed naturally. Although lithotripsy usually requires anesthesia and causes acute injury to the kidney, the total trauma is less than that of surgery. Lithotripsy is also under investigation as a treatment for gall stones and for certain other conditions [7].

In this article we consider *extracorporeal* lithotripsy.[1] As indicated in Figure 1, the patient is immersed in a water tank which contains a shock-wave generator and an ellipsoidal reflector. The generator is located at one focus of the reflector, and the patient is placed so that the stone is located at the other focus. An expanding spherical shock wave, initiated at the generator, is converted by reflection into a converging shock wave focused on the stone. In a typical treatment, several thousand shocks are administered at a rate of approximately one per second [3].

As we shall see below, lithotripsy pulses induce cavitation,[2] and there is evidence [8] that the resulting bubbles play an important role in breaking up stones.

*Received by the editors April 21, 1997; accepted for publication May 9, 1997.
http://www.siam.org/journals/sirev/40-2/32263.html

†Mechanical Engineering and Center for Nonlinear and Complex Systems, Duke University, Durham, NC (leh@me1.egr.duke.edu). The research of this author was partially supported by grant PRF 31645-G9 of the Petroleum Research Fund.

‡Department of Mathematics and Center for Nonlinear and Complex Systems, Duke University, Durham, NC (dgs@math.duke.edu). The research of this author was supported by NSF grant DMS-9504577.

§Department of Mathematics and Center for Research in Scientific Computation, North Carolina State University, Raleigh, NC (shearer@math.ncsu.edu). This author is adjunct professor of Mathematics at Duke University. His research was supported by NSF grant DMS-9504583 and by ARO grant DAAH04-94-G-0043.

¶Mechanical Engineering, Duke University, Durham, NC (pz1@me1.egr.duke.edu). The research of this author was supported by the Whitaker Foundation and by NIH grant PO1-DK20543.

[1]In *intracorporeal* lithotripsy a microprobe, inserted into the patient's body, is used to generate shock waves adjacent to the stone.

[2]The spontaneous formation of bubbles in a liquid experiencing tensile stress was called *cavitation* by Froude. The possibility of cavitation was first predicted theoretically by Euler in 1754. In the late nineteenth century, cavitation bubbles were observed behind the rapidly spinning propellers of large ships. In 1917, Rayleigh [24] published the first theoretical study of cavitation; this paper, part of the war effort, arose from trying to understand the catastrophic destruction of ship propellers.

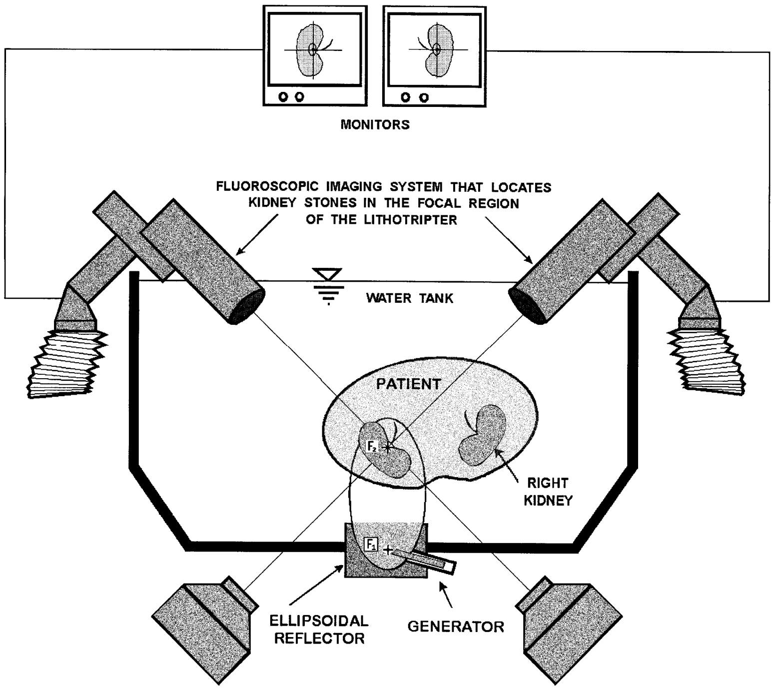

Fig. 1.

In this paper we focus on the dynamics of a single bubble reacting to an incident ultrasound pulse.[3] Specifically, in section 2 we formulate this problem in terms of Rayleigh's theory [24]; in section 3 we analyze bubble oscillations according to this theory in the asymptotic limit of large oscillations; and in sections 4 and 5 we briefly discuss some of the effects neglected in the simple theory.

In writing this article we hope

- to make a beautiful real-world application of mathematics more readily available to mathematicians,
- to illustrate for nonmathematicians the usefulness of mathematical techniques in these problems, and
- to publicize an innovative course format that may be of general interest.

Regarding the first goal, the paper provides a brief overview, with references, of mathematical problems in lithotripsy. Regarding the second goal, in section 3 we illustrate the power of scaling and asymptotic methods in an oversimplified case chosen for pedagogical reasons; of course these techniques, which do not require numerical sim-

Although cavitation seems well grounded in everyday experience—one knows that water is pulled apart by tensile stresses—analysis of this phenomenon is rather subtle. Statistical mechanics predicts that the tension needed to rupture a *homogeneous* liquid is nearly as great as that needed to rupture a solid. However, inhomogeneities in a real liquid, which serve as nucleation centers for rupture, immensely reduce its tensile strength. Purification decreases inhomogeneities and therefore increases tensile strength somewhat, but quantitative predictions are difficult. Fortunately, as we shall justify in section 4.3, for lithotripsy one need study only the response of a *pre-existing* bubble to an ultrasound pulse, a much simpler problem than bubble initiation.

[3]This is one aspect of a larger question: what functional of the applied pressure pulses quantifies the damage to a stone, and what functional quantifies damage to the surrounding tissue? Answers to this larger question might suggest ways to improve lithotripsy dramatically.

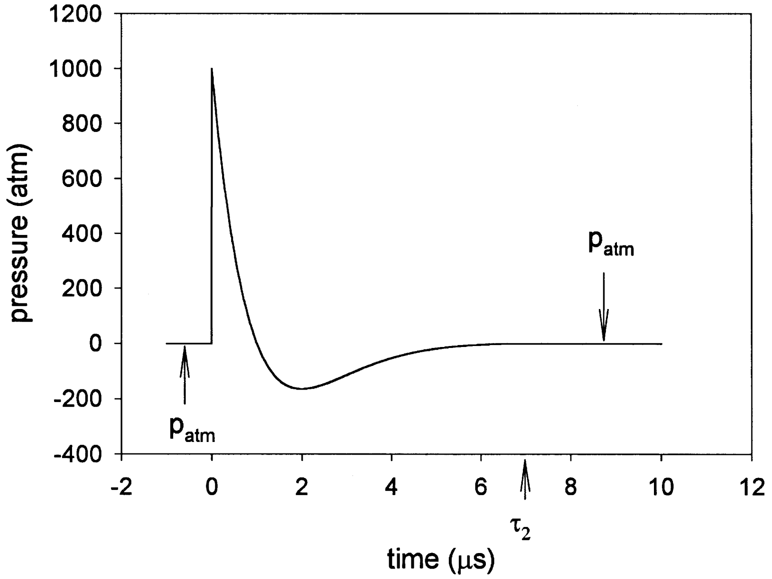

FIG. 2.

ulations, could also be applied to more realistic cases. Regarding the third goal, the present collaboration between two mathematicians and two engineers was fostered by a graduate course in the Mathematics Department; we discuss this course in an appendix.

2. Bubble dynamics according to Rayleigh's theory. Figure 2 shows the pressure pulse delivered to the second focus of the ellipsoidal reflector in a lithotripter tank, as a function of time. (Actually, because of defocusing due to nonlinear wave interactions [5], more or less the same pressure occurs over a neighborhood of the focus that is a few millimeters in diameter.) The most noteworthy feature of this graph is that, although the pulse begins with compression, as one expects, this is followed by *tension.*[4] The wave form is usually modeled as (a portion of) an exponentially modulated oscillation:

$$p(t) = \begin{cases} 2P_0\, e^{-t/\tau_1} \cos(t/\tau_2 + \pi/3) \,+\, p_{atm}, & 0 < t < (7\pi/6)\tau_2, \\ p_{atm} & \text{otherwise,} \end{cases} \tag{2.1}$$

where p_{atm} denotes atmospheric pressure and

$$\begin{aligned} &\text{(a)} \quad 200p_{atm} \le P_0 \le 1000p_{atm}, \\ &\text{(b)} \quad \tau_1 \approx 1.1\,\mu sec, \\ &\text{(c)} \quad \tau_2 \approx 1.9\,\mu sec. \end{aligned} \tag{2.2}$$

Note that because of the phase shift by $\pi/3$ in (2.1), the maximum of the first term in (2.1) is only P_0. Here the arrival of the pulse is modeled as a jump discontinuity; the actual rise time is a few nanoseconds.

[4]Precisely what causes this tension is not known. There is speculation, including some supporting experimental evidence [12], that diffractive effects at the edge of the ellipsoidal reflector are responsible.

Rayleigh [24] studied the dynamic response of an isolated bubble to changing pressure levels, especially tension. Specifically, he considered a spherical bubble in an incompressible fluid which is subjected to a spatially uniform pressure $p_\infty(t)$ at infinity such as that given by (2.1): in mathematical terms, the pressure $p(r,t)$ in the incompressible Navier–Stokes equation must satisfy the boundary condition

$$\lim_{r\to\infty} p(r,t) = p_\infty(t). \tag{2.3}$$

At first blush Rayleigh's theory would seem totally inappropriate for the present context. Indeed, in lithotripsy, pressure is delivered to the stone via a converging spherical wave; wave propagation of course requires compressibility, and the spatial variation in a converging spherical wave, seemingly inconsistent with the assumption of uniform pressure at infinity, concentrates enormous pressures near the kidney stone without undue damage to surrounding tissue. However, regarding spatial variation: a bubble typically has an initial radius of a few microns while the "focal region" over which maximum pressures occur has a radius of a few millimeters, three orders of magnitude greater than R_0. Similarly, regarding compressibility, or equivalently, finite speed of propagation: a sound wave can travel a distance equal to a bubble radius in the time

$$\frac{R_0}{c} \approx \frac{3\times 10^{-6}\, m}{1.5\times 10^{3}\, m/sec} = 2\, nsec,$$

while the pressure pulse (2.1) evolves over a characteristic time on the order of $10\mu sec$, again several orders of magnitide greater. Thus the Rayleigh theory appears relevant for lithotripsy.

We now begin the mathematical formulation of bubble dynamics. Consider spherically symmetric motion of an inviscid, incompressible liquid occupying the exterior of a spherical air bubble of varying radius $R(t)$. The liquid velocity $v(r,t)$ and pressure $p(r,t)$ satisfy the incompressible Euler equations in the region $\{R(t) < r < \infty\}$,

$$\begin{aligned} &\text{(a)} \quad \rho(\partial_t v + (v\cdot\nabla)v) = -\nabla p,\\ &\text{(b)} \quad div\, v = 0, \end{aligned} \tag{2.4}$$

where ρ is the (constant) density of the liquid. At infinity we impose the boundary condition (2.3), assuming

$$p_\infty(t) \equiv p_{atm} \quad \text{for} \quad t < 0. \tag{2.5}$$

At the moving liquid/bubble interface we impose two boundary conditions: a kinematic boundary condition

$$v(R(t),t) = \dot{R}(t)\hat{r}, \tag{2.6}$$

where $\hat{r}$ is a unit vector in the radial direction, and a pressure boundary condition

$$p(R(t),t) = p_{atm}[R_0/R(t)]^{3\gamma}, \tag{2.7}$$

where $\gamma = 1.4$ is the adiabatic exponent. As discussed in Chapter 2 of Brennen [1], boundary conditions (2.6, 2.7) may be derived from the following assumptions:

- For $t < 0$, the static air bubble of radius R_0 is in equilibrium with the surrounding liquid at atmospheric pressure. (Surface tension and the partial pressure of water vapor in the bubble are neglected.)

- During the entire motion, the gas in the bubble maintains a spatially uniform temperature and density described by the ideal-gas law. (In particular, the momentum of the gas is neglected.)
- No heat or dissolved gas is exchanged between the liquid and bubble.

These approximations will be examined in sections 4 and 5.

Following Rayleigh [24], we reduce this moving-boundary problem for the Euler equations to an ordinary differential equation (ODE) for the bubble radius $R(t)$. By the incompressibility condition (2.4b), $v(r,t)$ has the form

$$v = \frac{u(t)}{r^2}\hat{r}, \tag{2.8}$$

and (2.6) relates the arbitrary function of time $u(t)$ in (2.8) to $R(t)$:

$$v(r,t) = \frac{R^2(t)\dot{R}(t)}{r^2}\hat{r}. \tag{2.9}$$

On substituting (2.9) into the momentum equation (2.4a), integrating with respect to r from $R(t)$ to ∞, and invoking (2.3) and (2.7), we deduce that

$$\rho\left[R\ddot{R} + \frac{3}{2}\dot{R}^2\right] = p_{atm}(R_0/R)^{3\gamma} - p_\infty(t), \tag{2.10}$$

which is a special case of what is called the Rayleigh–Plesset equation.[5]

In Figure 3 is shown a numerical solution[6] of (2.10) assuming that $R_0 = 3\mu m$ and $p_\infty(t)$ is given by (2.1) with $P_0 = 1000\, p_{atm}$. Note that initially the bubble contracts in response to compression from $p_\infty(t)$; then it expands greatly during the tensile phase of $p_\infty(t)$ and *keeps the expanded radius long after* $p_\infty(t)$ *has returned to atmospheric pressure*;[7] finally it collapses very rapidly indeed.[8] (In the present theory, which neglects dissipation, the oscillations continue indefinitely; see section 4 regarding dissipative effects.) In the next section we study these free oscillations with analytical techniques.

3. Large-amplitude asymptotics.

We assume there is a time after which

$$p_\infty(t) \equiv p_{atm},$$

and we study the free oscillations of (2.10) for times after the perturbing pulse has returned to atmospheric pressure. Then (2.10) reduces to the autonomous equation

$$R\ddot{R} + \frac{3}{2}\dot{R}^2 = a^2\left[\left(\frac{R_0}{R}\right)^{3\gamma} - 1\right], \tag{3.1}$$

where

$$a = \sqrt{p_{atm}/\rho} \approx 10\, m/sec. \tag{3.2}$$

[5] More accurately, the Rayleigh–Plesset equation includes other effects, as in our equation (4.1) below.

[6] We are indebted to Mark Murray for performing these and other calculations mentioned below.

[7] High-speed photography provides experimental confirmation [30] for this behavior.

[8] To handle the numerical difficulties posed by rapid collapse, we used a variable-time-step integrator in solving (2.10).

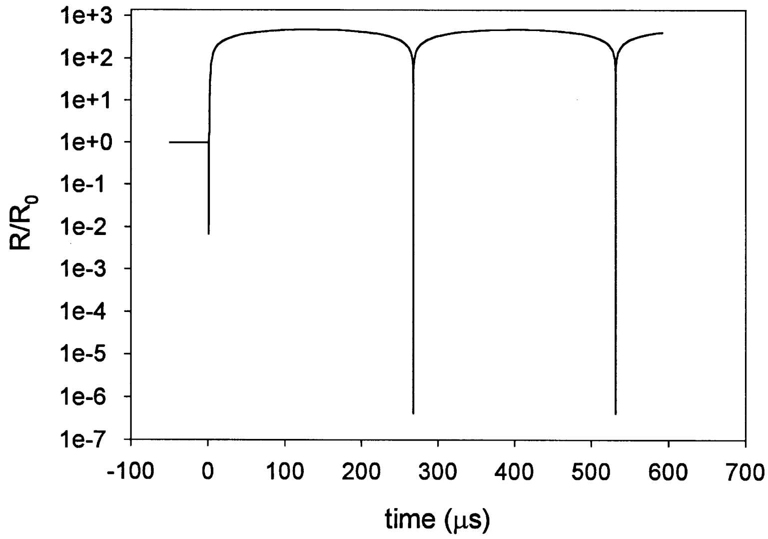

FIG. 3.

Note that a has units of velocity; quantitatively, $a \approx 0.007\,c$, where c is the speed of sound in water. We consider initial conditions for (3.1)

$$\text{(3.3)} \qquad \begin{array}{ll} \text{(a)} & R(0) = AR_0, \\ \text{(b)} & \dot{R}(0) = 0. \end{array}$$

If $A \approx 1$ in (3.3a), then the solution of (3.1) consists of small oscillations around the equilibrium at $R = R_0$ with period approximately $2\pi R_0/a\sqrt{3\gamma}$. (If $R_0 \approx 3\,\mu m$, the period in dimensional time is approximately $0.9\mu sec.$) Our goal is to analyze the oscillations of (3.1, 3.3) asymptotically in the limit $A \to \infty$. In particular, we (i) show that the period of large-amplitude oscillations is approximately proportional to A and (ii) estimate the maximum velocity of the bubble surface during collapse.

Multiplying (3.1) by the integrating factor $R^2\dot{R}$, we deduce that

$$\text{(3.4)} \qquad E = \frac{1}{2}R^3\dot{R}^2 + \frac{a^2}{3}R^3 + \frac{a^2}{3(\gamma-1)}\frac{R_0^{3\gamma}}{R^{3(\gamma-1)}}$$

is a constant of the motion. The first term in (3.4) represents the kinetic energy of the moving liquid in the region $\{R(t) < r < \infty\}$, as may be seen by integrating (2.9); the second term represents the potential energy of work done against atmospheric pressure at infinity; and the third term represents the internal energy of the gas in the bubble. The phase-plane trajectory of (3.1, 3.3) is a periodic orbit around a level set of the function E, as sketched in Figure 4 for the case $A = 2.5$. (A larger value of A would be better for the asymptotics but would greatly distort the graphs in Figures 4–6.) Note that this level set intersects the R-axis at two points: at $R = AR_0$, as given in (3.3), and at a second point that we shall denote[9] R_{min}. If we define t_{hp}

[9]We could estimate R_{min} from conservation of energy, and in fact we will do so below. For the time being, however, we carry R_{min} as an undetermined parameter since this is more typical of matched-asymptotic calculations.

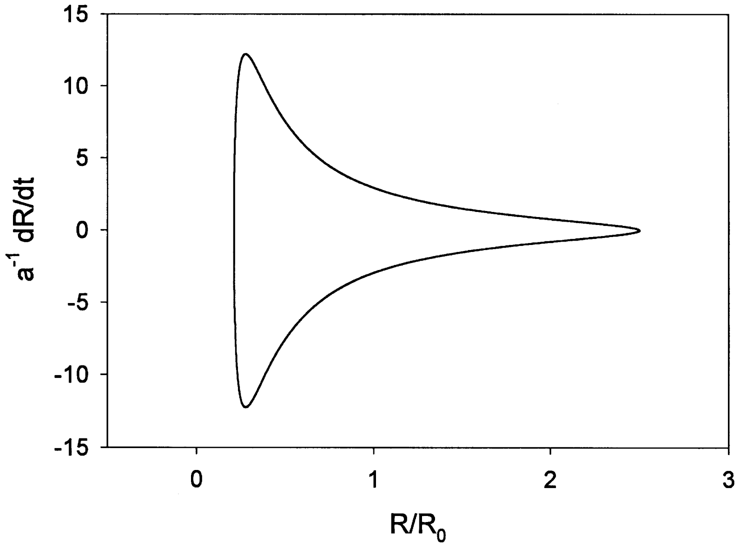

FIG. 4.

as the smallest (positive) time such that

$$R(t_{hp}) = R_{min}, \tag{3.5}$$

then the period T of the oscillations is given by

$$T = 2t_{hp}; \tag{3.6}$$

indeed, in recognition of this relationship, the subscript hp is mnemonic for "half-period."

We study (3.1, 3.3) by means of the first-order equation derived from conservation of energy. If R is large compared to R_0, we may neglect the third term in (3.4), which leads to the approximate problem

$$\text{(3.7)} \qquad \begin{array}{ll} \text{(a)} & R^3\dot{R}^2/2 + a^2R^3/3 = a^2A^3R_0^3/3, \\ \text{(b)} & R(0) = AR_0; \end{array}$$

here we have used the initial conditions (3.3) to evaluate the right-hand side (RHS) of (3.7a). We shall call the solution of (3.7) the *outer solution.*[10] The phase-plane trajectory of (3.7), again with $A = 2.5$, is shown in Figure 5. Comparing with Figure 4, we see that (3.7) captures much of the trajectory (3.1, 3.3) but breaks down as R gets small; specifically, the outer approximation predicts that R collapses to zero radius while $\dot{R}$ tends to ∞. As we will show below in our analysis of the inner solution, the neglected third term in (3.4) stops the collapse at a positive radius and limits the growth of $\dot{R}$ to finite, but very large, values.

[10]Although the geometry of this problem might suggest that *outer* and *inner* refer to the dependent variable R, these terms refer to domains in the *independent* variable t. Specifically, the outer solution, valid for most of the period of oscillation, describes the slow transition from large bubble radius to the threshold of collapse, while the inner solution, valid only for a brief interval, describes the bubble motion during the final stages of collapse.

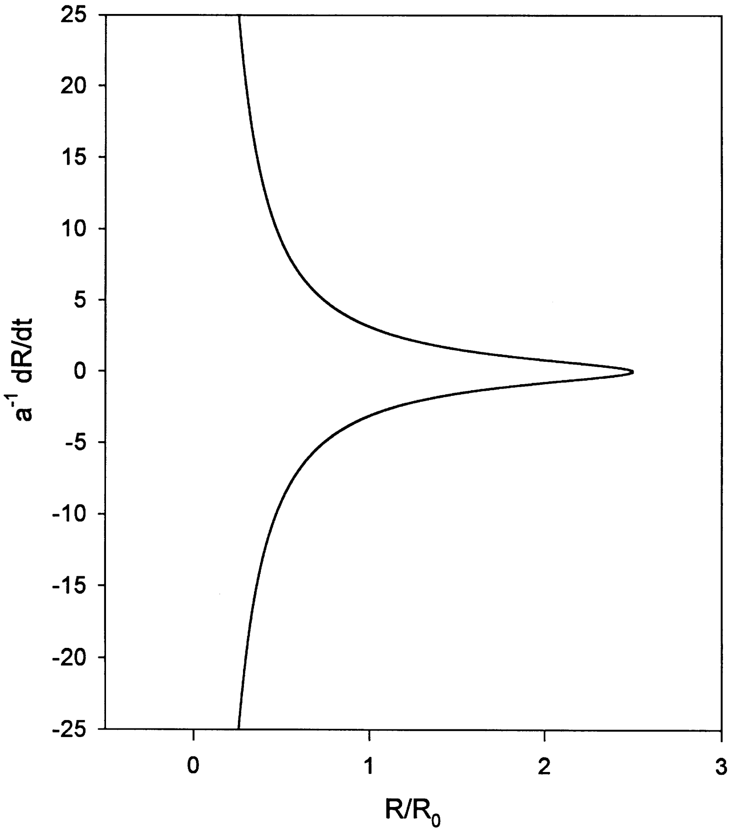

FIG. 5.

Despite this breakdown, we can use the outer solution to estimate asymptotically the period T of the oscillations. We introduce rescaled, dimensionless variables into (3.7):

$$y = \frac{R}{AR_0}, \quad t_{out} = \frac{t}{\tau_1}, \tag{3.8}$$

where the time scale $\tau_1 = AR_0/a$ is chosen to balance the powers of A in the two terms on the left-hand (LHS) of (3.7); this yields

$$\begin{aligned} &\text{(a)} \quad \frac{1}{2}y^3\left(\frac{dy}{dt_{out}}\right)^2 + \frac{1}{3}y^3 = \frac{1}{3}, \\ &\text{(b)} \qquad\qquad y(0) = 1. \end{aligned} \tag{3.9}$$

Solving (3.9a) for dt_{out}/dy and integrating from $y = 0$ to $y = 1$, we deduce that the solution $y(t_{out})$ goes to zero when t_{out} equals

$$t_{out,bd} = \sqrt{3/2}\int_0^1 \frac{dy}{\sqrt{(y^{-3}-1)}} \approx 0.915. \tag{3.10}$$

In dimensional time, this breakdown occurs at

$$t_{bd} = \frac{AR_0}{a}t_{out,bd} \approx 0.915\,\frac{AR_0}{a}.$$

Regarding the half-period t_{hp} in (3.5), we claim that, to the leading order in A^{-1},

$$t_{hp} \sim t_{bd}. \tag{3.11}$$

The intuition behind this claim is that the outer solution is a valid approximation up to a short time before it breaks down. More precisely, it follows from the scaling of the inner solution below that t_{hp} equals t_{bd} modified by a correction that is higher order in A^{-1}. Thus, we obtain the estimate

$$T \sim 1.830\, AR_0/a$$

for the period of the oscillations of (3.1, 3.3). If $A = 480$ and $R_0 = 3\mu m$ (as in the oscillations shown in Figure 3), then we obtain $T \approx 263\mu s$, and this estimate agrees with the numerical solution to 3 figures. This period is 286 times longer than the small-amplitude period.

It is instructive to re-express the energy (3.4) in terms of the rescaled variables (3.8):

$$E = A^3 R_0^3 a^2 \left\{ \frac{1}{2} y^3 \left(\frac{dy}{dt_{out}} \right)^2 + \frac{1}{3} y^3 + \frac{A^{-3\gamma}}{3(\gamma - 1)} \frac{1}{y^{3(\gamma-1)}} \right\}.$$

This expression shows explicitly that the third term in the energy is a small perturbation[11] for large A except that it becomes singular in the limit $y \to 0$, which we now consider.

When R is small compared to R_0, we neglect the second term in (3.4) rather than the third. This leads to the inner approximation

$$(3.12) \qquad \begin{aligned} &\text{(a)} \quad \frac{1}{2} R^3 \dot{R}^2 + \frac{a^2}{3(\gamma - 1)} \frac{R_0^{3\gamma}}{R^{3(\gamma-1)}} = \frac{a^2}{3(\gamma - 1)} \frac{R_0^{3\gamma}}{R_{min}^{3(\gamma-1)}}, \\ &\text{(b)} \quad R(t_{hp}) = R_{min}. \end{aligned}$$

The phase-plane trajectory of (3.12) is shown in Figure 6. Comparing with Figure 4, we see that (3.12) captures the behavior of (3.1, 3.3) for small R but distorts the approach to this regime from large values of R.

In the usual matched-asymptotic analysis, one would solve (3.12), carrying R_{min} as an unspecified parameter, and then determine R_{min} by matching the two approximations in the overlap region: i.e., as $R/R_{max} \to 0$ in the outer solution (where $R_{max} = AR_0$) and as $R/R_{min} \to \infty$ in the inner solution. In the present problem, conservation of energy provides a shortcut: to the lowest order in A^{-1}, the RHSs of (3.7a) and (3.12a) equal the energy E along the orbit and hence equal one another. That is,

$$\frac{a^2}{3(\gamma - 1)} \frac{R_0^{3\gamma}}{R_{min}^{3(\gamma-1)}} \sim \frac{a^2}{3} A^3 R_0^3$$

so that, if $\gamma = 1.4$,

$$R_{min} \sim C A^{-5/2} R_0, \tag{3.13}$$

[11] One could derive the outer problem more systematically by rescaling variables *before* dropping the third term in the energy. The more informal procedure we have followed here allows us to proceed directly to the inner problem from (3.4) without needing to work through an intermediate scaling.

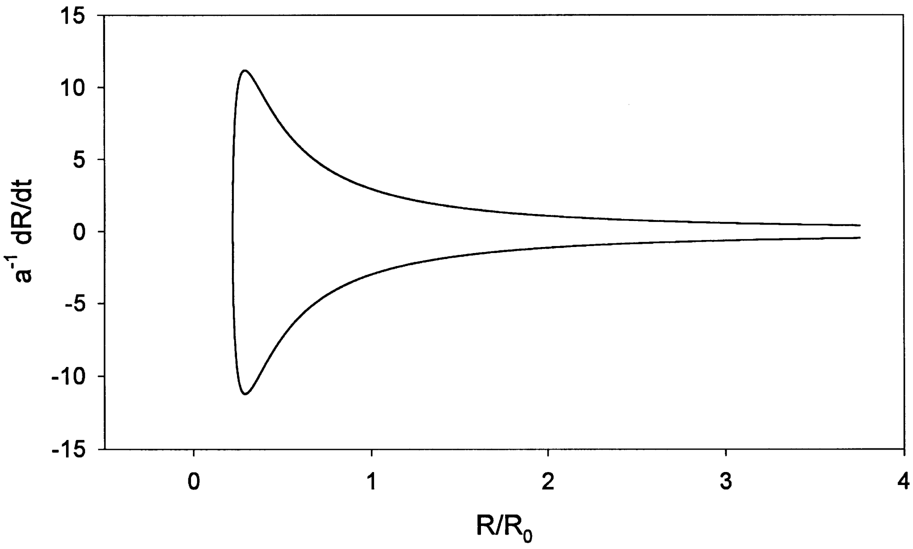

FIG. 6.

where $C = (\frac{2}{5})^{-5/6} \approx 2.146$. If $A = 480$, then (3.13) predicts $R_{min} \approx 4.25 \times 10^{-7} R_0$, while for the numerical solution $R_{min} \approx 4.26 \times 10^{-7} R_0$.

We may estimate the order of magnitide of V_{max}, the maximum collapse velocity, simply by appropriate scaling. We nondimensionalize (3.12) by substituting

$$z = \frac{R}{R_{min}}, \quad t_{in} = \frac{t - t_{hp}}{\tau_2},$$

where

$$\tau_2 = \left(\frac{R_{min}}{R_0}\right)^{(3\gamma+2)/2} \frac{R_0}{a} \tag{3.14}$$

is chosen to balance powers of R_{min}. One expects V_{max} to have the order of magnitude R_{min}/τ_2; thus, by (3.13, 3.14), if $\gamma = 1.4$, then $V_{max} \sim CA^{5.25}a$, where C is a dimensionless constant. To determine C we solve (3.12a) for $\dot{R}$ as a function of R and maximize this function to obtain

$$V_{max} \sim 0.0912 A^{5.25} a. \tag{3.15}$$

If $A = 480$, then (3.15) predicts $V_{max} \approx 1.09 \times 10^{13} a$, while the numerical solution $V_{max} \approx 1.08 \times 10^{13} a$. Although there is good agreement between these two results, this value for V_{max} is ridiculously large, on the order of 10^{11} times the speed of sound. Thus, a posteriori, we see that the incompressibility assumption in Rayleigh's theory is not even remotely justified. In section 4 we discuss several extensions of this model, including that of compressibility.

Incidentally, in the matching region both the inner and outer solution yield

$$R(t) \sim 1.33 A R_0 \left[\frac{a}{AR_0}(t_{hp} - t)\right]^{2/5}.$$

4. Neglected effects amenable to an ODE model.

4.1. Several minor effects. Generalizing Rayleigh's analysis, Plesset [19] studied a spherical bubble including surface tension and viscosity. As shown in Brennen [1], these effects can be modeled by changing (2.10) to

$$\rho\left[R\ddot{R}+\frac{3}{2}\dot{R}^2+4\nu\dot{R}/R\right]=p_{atm}(R_0/R)^{3\gamma}-p_\infty(t)+2S/R, \tag{4.1}$$

where $\nu = 10^{-6}\, m^2/sec$ is the kinematic viscosity of water and $S = 0.7\times 10^{-6}\, atm\cdot m$ is its surface tension.

The surface-tension term in (4.1) preserves the Hamiltonian structure of (2.10). Observe that

$$\left.\frac{d}{dR}(2S/R)\right|_{R=R_0}\left\{\left.\frac{d}{dR}p_{atm}(R_0/R)^{3\gamma}\right|_{R=R_0}\right\}^{-1}\approx\frac{1}{9}; \tag{4.2}$$

thus for small oscillations, the surface-tension term represents roughly a 10% correction to the RHS of (2.10). In both the limits $R\to\infty$ and $R\to 0$, the surface-tension term becomes much smaller than one of the other two terms on the right in (4.1); thus, for large-amplitude oscillations, surface tension is still less important.[12]

The viscosity term in (4.1) damps small oscillations exponentially; if $R_0 \approx 3\,\mu m$, the decay time is on the order of

$$R_0^2/\nu \approx 9\mu sec,$$

ten times longer than the period of one (small) oscillation. For large oscillations, as discussed in the next section, the nonlinear damping due to liquid compressibility is vastly more important than viscosity.

Similarly, one can model the effect of water vapor inside the bubble by including yet another term in (2.10). However, the physics underlying vapor pressure is less familiar—in particular, temperature is involved—so we refer to Brennen [1] without elaborating here.

4.2. Liquid compressibility. Using the incompressible Euler equations (2.4) to describe liquid motion, we have found collapse velocities vastly greater than the speed of sound c. Thus, one needs to allow for liquid compressibility. Although we reduced the free-boundary problem for (2.4) to the ODE (2.10) for the bubble radius $R(t)$, in the compressible case this reduction is not possible. However, several authors (e.g., [13, 16]) have shown that, asymptotically in v/c, such a reduction is possible.[13] Despite the fact that v/c is *not* small, we examine the predictions of these models.

In Figure 7 is shown the response of a $3\mu m$ bubble to the pressure pulse (2.1) with $P_0 = 1000p_{atm}$, computed according to the Gilmore equations. Comparing with Figure 3, we see that the predictions of the compressible and incompressible theories agree rather well before collapse but differ greatly during and after collapse.

[12] Less important for spherical bubbles, but see section 5 regarding surface tension and the loss of sphericity.

[13] For years it was mysterious that two different, valid approaches gave different equations for $R(t)$. Prosperetti and Lezzi [22] showed, via a systematic asymptotic expansion, that (i) to the leading order in v/c, the equations do agree and (ii) nevertheless, as a practical matter, the Gilmore formulation tends to give better accuracy.

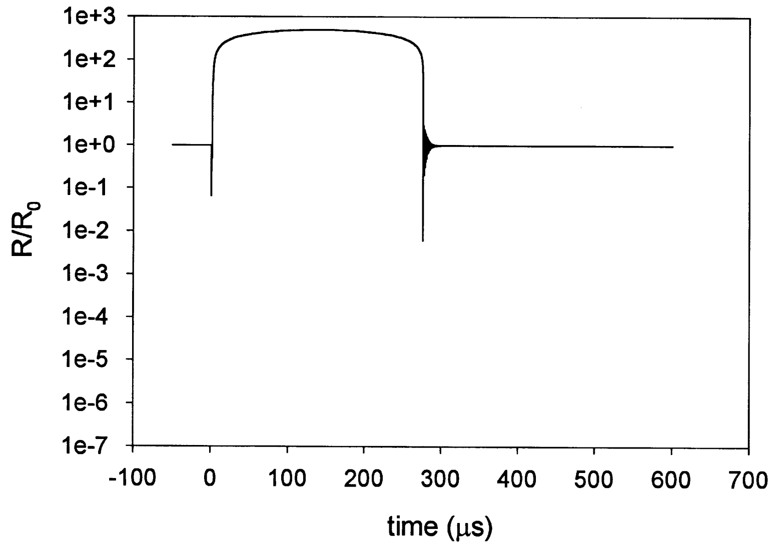

FIG. 7.

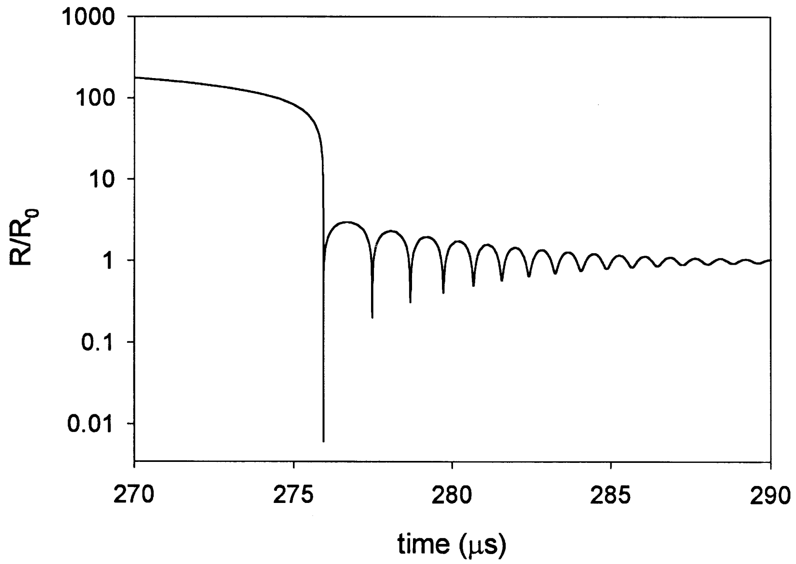

FIG. 8.

Specifically, (i) in the compressible case R_{min} is four orders of magnitude larger than in the incompressible case and (ii) in the compressible case the oscillations following collapse are damped more rapidly than can be resolved on the scale of the figure. (To facilitate comparison, we have used the same scale in Figure 7 as in Figure 3; see Figure 8 for an expanded view of the ringing following collapse in Figure 7.) In the compressible case, the kinetic energy of the imploding liquid is converted to a radiated acoustic wave.

Keller and Kolodner [15] explained this behavior from phase-plane analysis. Equation (3.1) has a single equilibrium, a center, at $R = R_0$, $\dot{R} = 0$, and its orbits consist of closed trajectories encircling this point. Keller and Kolodner showed that, when first-order compressibility effects are included in (3.3), two changes result: (i) the center at $R = R_0$, $\dot{R} = 0$ is converted to a sink and (ii) another equilibrium, a saddle point, is introduced on the $\dot{R}$-axis. As illustrated in Figure 1 of [15], any trajectory starting on the R-axis, no matter how far out, will be "trapped" by the unstable orbit that emerges from the saddle point and spirals into the sink.

4.3. Gas diffusion. According to Henry's law [11], in an equilibrium situation consisting of water and gas phases separated by an interface, the water will contain a small amount of dissolved gas, the concentration being proportional to the pressure of the gas. For example, water in a lithotripter tank is in contact with the atmosphere, and as a result, in steady state, approximately 0.0025% of the liquid (by mass) consists of dissolved air molecules. Suppose that a bubble in the tank expands, thereby decreasing the pressure inside from its initial value of p_{atm}. Then the equilibrium of Henry's law is disturbed: i.e., the concentration of gas dissolved in water near the interface will be too high relative to the reduced pressure in the bubble. Consequently gas will diffuse from the liquid into the bubble, and reduced gas concentration near the interface will in turn lead to diffusion in the bulk of the liquid. For large-amplitude bubble oscillations, the departure from equilibrium is very great indeed: if the bubble radius increases a hundred-fold, then its volume increases a million-fold, and its pressure decreases correspondingly. Thus, although gas diffusion is a fairly slow process, it has a major impact on large-amplitude bubble dynamics.

If one makes the Plesset–Zwick [21] approximation that gas diffusion is confined to a boundary layer near the interface, one may reduce the moving-boundary problem to a system of ODE. Church [6] solved these ODEs numerically (also including compressibility) in the context of lithotripsy. He found that, after the arrival of the pulse, a bubble with $R_0 \approx 3\,\mu m$ re-equilibrates at a new radius approximately ten times larger that R_0, *a thousand-fold increase in volume.*[14] This expansion reflects the large amount of gas that enters the bubble during its expanded phase. The extra air in the bubble acts as a cushion that decreases the violence of collapse and slows the decay of oscillations following collapse.

5. Neglected effects requiring a PDE model. Expanding bubbles tend to remain approximately spherical, but collapsing bubbles are vulnerable to extreme distortion. In a collapsing bubble, small deviations from sphericity are amplified by the Rayleigh–Taylor instability [20, 26], which appears when a heavy fluid is accelerated into a light one. If many spherical harmonics $Y_{\ell m}$ are unstable, the bubble surface becomes very irregular, and the bubble may break up into a cluster of smaller bubbles. (See the photographs in Figure 3.3 on p. 71 of Brennen [1].) No one knows for certain how the formation of bubble clusters impacts lithotripsy: wave propagation in a bubbly liquid is notoriously difficult to analyze [27].

[14] Church's result helps us clarify an issue above. Although we derived (2.10) by assuming that $R(t) \equiv R_0$ for $t < 0$, in fact a small bubble is unstable to gas diffusion. Brennen [1] shows on p. 49 that a small bubble should decay to zero radius in a few seconds. This decay is due to surface tension: gas pressure inside the bubble is higher than p_{atm} by $2S/R$, and this overpressure, compared to the equilibrium of Henry's law, causes gas to continually diffuse out of the bubble into the liquid.

Nevertheless, in lithotripsy, the assumption of a pre-existing bubble is still appropriate: the first lithotripsy pulse creates cavitation bubbles that, according to Church's result, fill up with enough air so that they do not diffuse away before the arrival of the next pulse a second later, and so on with subsequent pulses. (This is an example of what is called *rectified diffusion*: see the discussion in section 4.9 of Brennen.)

In some cases, because of the stabilizing influence of surface tension, no or only a few spherical harmonics are unstable. Figures 3.4–3.6 on pp. 72–73 of Brennen [1] illustrate cases where instability occurs only in the modes with $\ell = 2$. This case is particularly significant when a nearby wall breaks spherical symmetry: the instability may grow to a "re-entrant jet" which strikes hard against the wall. Such jets are an important, perhaps the dominant, mechanism for breaking up stones [28, 29].

It is not clear just how extreme the conditions inside a collapsing bubble can become. Conditions are sufficiently extreme for the gas in the bubble to emit light—sonoluminesence has been known for over sixty years.[15] Putterman [23] suggested that they may be sufficiently extreme to make *fusion* possible! However, it *is* clear that, even in the spherically symmetric case, the interior of a collapsing bubble is far from spatially uniform. Indeed, intense shock waves may be generated inside the bubble by its collapse at hypersonic speeds [23]. Similarly, as shown by the computation of Hickling [14] and of others (see p. 70 of Brennen [1]), temperature gradients inside a collapsing bubble are so steep that, despite the brevity of collapse, significant heat is conducted away from the bubble.

Incidentally, partial differential equation (PDE) models are also needed to assess the adequacy of ODE models that include liquid compressibility and gas diffusion (cf. section 4).

Appendix: An interdisciplinary course[16] in a mathematics department. The story of the course behind the present collaboration, which I taught in the spring of 1996, began in the fall of 1995 with a slightly audacious act: I sent a memo to all the science and engineering faculty at Duke asking if they would like the assistance of a group of math graduate students working on mathematical problems arising in their (the faculty member's) research. I proposed to teach math students about real-world applications of mathematics through a case-study course focused on such a problem. The response to the memo included a half dozen *excellent* problem areas, from which I chose[17] lithotripsy.

In broad terms, during the first half of the course I lectured on scientific and mathematical background for the problem, and during the second half two student[18] teams did independent research[19] with my collaboration on problems we had isolated earlier. (I say "with my collaboration" rather than "under my supervision" because I was very aware that others had far more knowledge of nonmathematical aspects of the problem than I.) Classroom time in the second half of the semester was divided approximately equally between research conferences with the two teams, student lectures (some on homework problems, others on the results of their research), and further lectures on background by me.[20]

[15]This subject is surveyed in [9]. See also [2, 17] for interesting new ideas on the problem.

[16]This course was taught by DGS, the narrator in this appendix.

[17]For the course I offered in the spring of 1997, I changed the selection procedure slightly: I narrowed the choice to *three* problems, asked the proposers to summarize their problems in 15-minute lectures to the graduate students, and then included student response to the lectures in making the final choice.

[18]In addition to the math students, the course was attended by four graduate students in engineering, their advisors (on the engineering faculty) who proposed the problem, and two math faculty; here the term "student" includes all of these.

[19]The work of one team led to publishable research [18]. It concerns a model for tissue damage during lithotripsy.

[20]The course was described in more detail in the Duke newspaper; this article is available on the web at http://www.dukenews.duke.edu/Dialogue/schaeffer.531, which can be accessed through my home page. The article [25] describes an earlier version from which the present course evolved.

I believe a math course in this format has benefits (i) for math students, (ii) for applied scientists, (iii) for the mathematics profession, and (iv) for the teacher. Regarding (i), math students gain experience in collaborating with applied scientists; this broadening of experience addresses one of the major challenges facing graduate education in mathematics [10]. Regarding (ii), challenging mathematical problems arise frequently in an applied research projects, and a mathematician's expertise and different point of view may contribute to more rapid progress in the work. Regarding (iii), progress resulting from such collaborations may help demonstrate the usefulness of mathematics for the world-at-large, an important issue in the present applications-oriented political climate. Regarding (iv), I find the scientific contact with applied scientists very stimulating intellectually, and I am delighted that I can achieve this within the context of my existing teaching responsibilities.

REFERENCES

[1] C. Brennen, *Cavitation and Bubble Dynamics*, Oxford University Press, Oxford, UK, 1995.

[2] M. Brenner, S. Hilgenfeldt, D. Lohse, and R. Rosales, *Acoustic-energy storage in single-bubble sonoluminescence*, Phys. Rev. Lett., 77 (1996), pp. 3467–3470.

[3] C. Chaussy and G. Fuchs, *Current state and future developments of noninvasive treatment of human urinary stones with extracorporeal shock wave lithotripsy*, J. Urology, 141 (1989), pp. 782–789.

[4] C. Chaussy, E. Schmiedt, D. Jocham, W. Brendel, B. Forssmann, and V. Walther, *First clinical experience with extracorporeally induced destruction of kidney stones by shock waves*, J. Urology, 127 (1982), pp. 417–420.

[5] T. Christopher, *Modeling the Dornier HM*3 *lithotripter*, J. Acoustical Soc. America, 96 (1994), pp. 3088–3095.

[6] C.C. Church, *A theoretical study of cavitation generated by an extra corporeal shock-wave lithotripter*, J. Acoustical Soc. America, 86 (1989), pp. 215–227.

[7] A.J. Coleman and J.E. Saunders, *A review of the physical properties and biological effects of the high-amplitude acoustic field used in extracorporeal lithotripsy*, Ultrasonics, 31 (1993), pp. 75–89.

[8] A.J. Coleman, J.E. Saunders, L.A. Crum, and M. Dyson, *Acoustic cavitation generated by an extracorporeal shockwave lithotripter*, Ultrasound in Medicine and Biology, 13 (1987), pp. 69–76.

[9] L. Crum, *Sonoluminescence*, Physics Today, Sept. 1994, pp. 22–29.

[10] R. Douglas, H. Bass, A. Friedman, P. Glynn, R. Graham, R. Hughes, R. Jacob, P. Langenberg, D. Lewis, J. S. Long, J. Rice, D. Richards, K. Uhlenbeck, and M. Wheeler, *Educating Mathematical Scientists: Doctoral Study and the Postdoctoral Experience in the United States*, Report to the National Research Council, National Academy Press, Washington, D. C., 1992.

[11] A. Eller and H.G. Flynn, *Rectified diffusion during nonlinear pulsations of cavitation bubbles*, J. Acoustical Soc. America, 37 (1965), pp. 493–503.

[12] W.S. Filler, *Shock-beaming capabilities of hydrodynamic conical shock tubes*, J. Acoustical Soc. America, 50 (1970), pp. 1313–1320.

[13] F. Gilmore, *The Growth of Collapse of a Spherical Bubble in a Viscous Compressible Liquid*, Tech. Rep. 26-4, Hydrodynamics Laboratory, California Institute of Technology, Pasadena, CA, April 1952.

[14] R. Hickling, *Effects of thermal conduction in sonoluminescence*, J. Acoustical Soc. America, 35 (1963), pp. 967–974.

[15] J. Keller and I. Kolodner, *Damping of underwater explosion bubble oscillations*, J. Appl. Physics, 27 (1956), pp. 1152–1161.

[16] J.B. Keller and M. Miksis, *Bubble oscillations of large amplitude*, J. Acoustical Soc. America, 68 (1980), pp. 628–633.

[17] D. Lohse, M. Brenner, T. Dupont, S. Hilgenfeldt, and B. Johnston, *Sonoluminescing air bubbles rectify argon*, Phys. Rev. Lett., 78 (1997), pp. 1359–1362.

[18] M. Murray, H. Tong, L. Howle, and P. Zhong, *Response of a cavitation bubble surrounded by a viscoelastic membrane*, Paper number FEDSM97-3437 (on CD Rom) Proc. Biomedical Fluid Engineering Symposium II, Vancouver, BC, Canada, 1997.

[19] M.S. Plesset, *The dynamics of cavitation bubbles*, ASME J. Appl. Mech., 16 (1949), pp. 228–331.
[20] M.S. Plesset, *On the stability of fluid flows with spherical symmetry*, J. Appl. Physics, 25 (1954), pp. 96–98.
[21] M.S. Plesset and S.A. Zwick, *A nonsteady heat-diffusion problem with spherical symmetry*, J. Appl. Physics, 23 (1952), pp. 95–98.
[22] A. Prosperetti and A. Lezzi, *Bubble dynamics in a compressible liquid. Part* 1. *First-order theory*, J. Fluid Mech., 186 (1986), pp. 457–478.
[23] S.J. Putterman, *Sonoluminescence: Sound into light*, Scientific American, Feb. 1995, pp. 46–51.
[24] L. Rayleigh, *On the pressure developed in a liquid during the collapse of a spherical cavity*, Phil. Mag., 34 (1917), pp. 94–98.
[25] D. Schaeffer, *Memoirs from a small-scale course in industrial math*, Notices Amer. Math. Soc., 43 (1996), pp. 550–557.
[26] D.H. Sharp, *An overview of Rayleigh-Taylor instability*, Phys. D, 12 (1984), pp. 3–18.
[27] M. Watanabe and A. Prosperetti, *Shock waves in dilute bubbly liquids*, J. Fluid Mech., 274 (1994), pp. 349–381.
[28] P. Zhong and C.J. Chuong, *Propagation of shock waves in elastic solids caused by the impact of cavitation microjets. Part* I: *Theoretical formulation*, J. Acoustical Soc. America, 94 (1993), pp. 19–28.
[29] P. Zhong, C.J. Chuong, and G.M. Preminger, *Propagation of shock waves in elastic solids caused by the impact of cavitation microjets. Part* II: *Application of extracorporeal shock-wave lithotripsy*, J. Acoustical Soc. America, 94 (1993), pp. 29–36.
[30] P. Zhong, I. Cioanta, F.H. Cocks, and G.M. Preminger, *Inertial cavitation and associated acoustic emission produced during electrohydraulic shock-wave lithotripsy*, J. Acoustical Soc. America, 101 (1997), pp. 2940–2950.